ACS NANO

www.acsnano.org

Generalizable Organic-to-Aqueous Phase Transfer of a Au_{18} Nanocluster with Luminescence Enhancement and Robust Photocatalysis in Water

Zhongyu Liu[1], Yitong Wang[1], Weijie Ji[1], Xiaowei Ma[1], Christopher G. Gianopoulos[2], Sebastian Calderon[3], Timothy Ma[1], Lianshun Luo[1], Abhrojyoti Mazumder[1], Kristin Kirschbaum[2], Elizabeth C. Dickey[3], Linda A. Peteanu,[1] Dominic Alfonso,[4]* and Rongchao Jin[1]*

[1]Department of Chemistry, Carnegie Mellon University, Pittsburgh, Pennsylvania 15213, USA

[2]Department of Chemistry and Biochemistry, University of Toledo, Toledo, Ohio 43606, USA

[3]Department of Materials Science and Engineering, Carnegie Mellon University, Pittsburgh, Pennsylvania 15213, USA

[4]National Energy Technology Laboratory, United States Department of Energy, Pittsburgh, Pennsylvania 15236, USA

ACS Nano

February 28, 2025

TOC

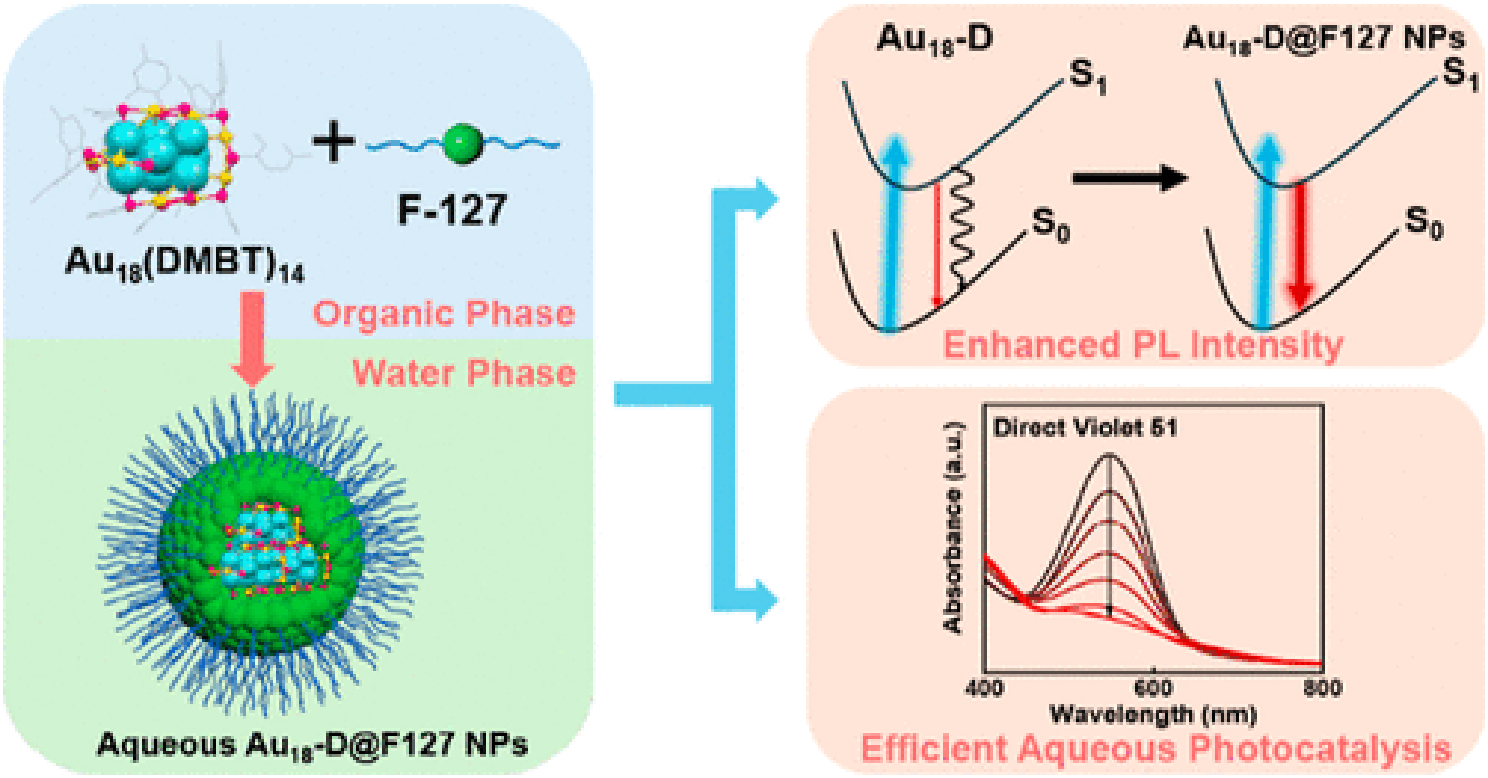
Au18(DMBT)14
F-127
Organic Phase
Water Phase
Aqueous Au18-D@F127 NPs
Au18-D
S1
S0
Au18-D@F127 NPs
S1
S0
Enhanced PL Intensity
Direct Violet 51
Absorbance (a.u.)
400
600
800
Wavelength (nm)
Efficient Aqueous Photocatalysis

Pluronic F127

Triblock copolymer, poly(ethylene oxide)-poly(propyleneoxide)-poly(ethylene oxide)

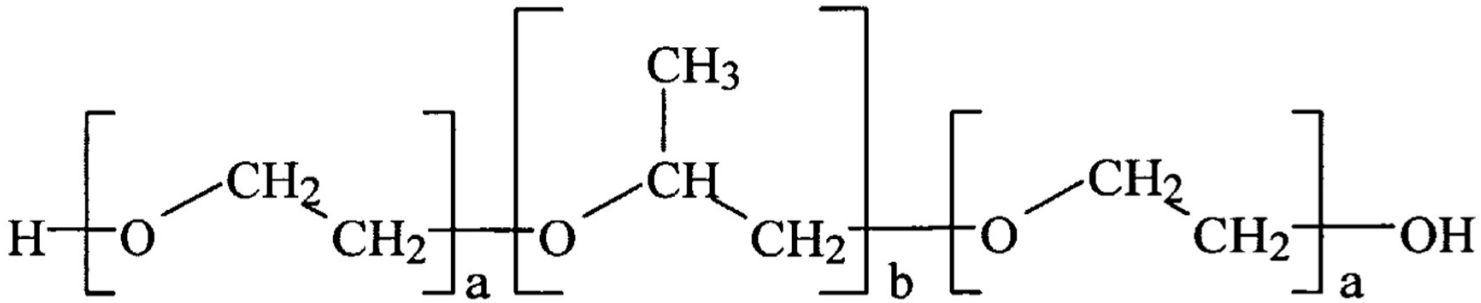

PEO PPO PEO

- Chemical structure of Pluronic F-127,where a = 100 and b=65 denote the number of ethylene oxide and propylene oxide monomers per block

Shaikhullina, M. et al., *J. Mol. Liq.* ***2020***, *306*, 112898.

Importance of the work

- Organic-to-aqueous phase transfer of gold cluster, rendering water solubility and biocompatibility
- During phase transfer, cluster's structure, electronic and optical features remain altered
- Presents it as general strategy extending to different gold clusters
- Photocatalytic activation of persulfate ions and photodegradation of water pollutants efficiently

Relevance to our group

- Organic soluble gold and silver clusters in our laboratory
- Direction towards PL enhancement of our clusters

Synthesis and purification

Metal(I)-thiolate reduction in presence of $NaBH_4$

78.99 mg of $HAuCl_4 \cdot 3H_2O$ and **136.7 mg TOAB (0.25 mmol)** were dissolved in 15 ml of THF under rapid stirring (~1000 rpm). The solution turned to deep orange in 30 minutes. Then, **DMBT (138 µL)** was added into the reaction mixture under ice bath. Subsequently, **Et_3N (70 µL)** was added all at once, and the stirring speed was reduced to ~100 rpm. After 30 min, a freshly prepared aqueous solution of **$NaBH_4$ (47.5 mg, 1.25 mmol, 2 mL)** was added dropwise to the reaction solution over a period of 5 minutes. Then, the stirring speed was raised to ~500 rpm. The reaction was allowed to proceed for 8 hours under 0 °C condition. After the reaction, the solvent was rotary evaporated, giving rise to a dark oil-like liquid. The oil was precipitated with methanol and the precipitate was washed by excess methanol.

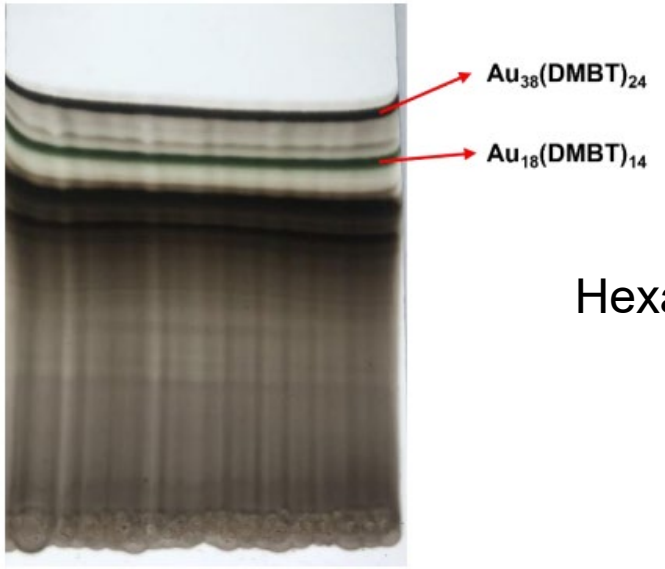

Hexane : DCM = 1:1

Figure S1. TLC separation of $Au_{18}(DMBT)_{14}$ from the product mixture.

Characterization of Au_{18}

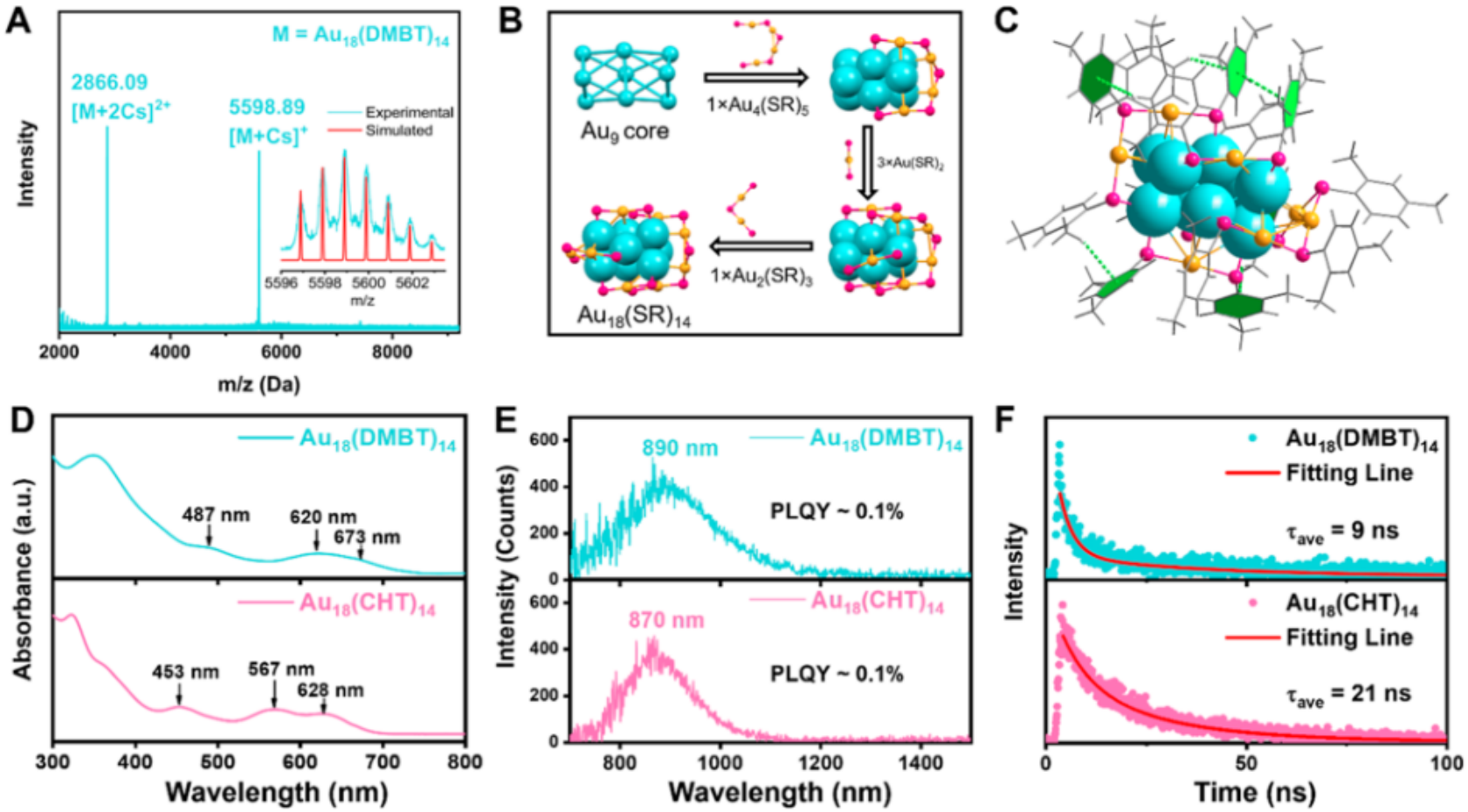

Figure 1. (A) ESI mass spectrum of $Au_{18}(DMBT)_{14}$ (CsOAc was added to facilitate ESI analysis); inset shows the experimental isotope pattern (blue profile) of m/z at 5598.89 and the theoretical pattern (red). (B) Anatomy of the X-ray structure of $Au_{18}(DMBT)_{14}$ NC. (C) Illustration of intramolecular $\pi-\pi$ interaction and C−H−π interaction in $Au_{18}(DMBT)_{14}$. (D) UV−vis absorption spectra of $Au_{18}(DMBT)_{14}$ (upper panel) and $Au_{18}(CHT)_{14}$ (bottom panel). (E) PL spectra of $Au_{18}(DMBT)_{14}$ (upper panel) and $Au_{18}(CHT)_{14}$ (bottom). (F) PL decay curves of $Au_{18}(DMBT)_{14}$ (upper panel) and $Au_{18}(CHT)_{14}$ (bottom).

Characterization of Au_{18}@F127

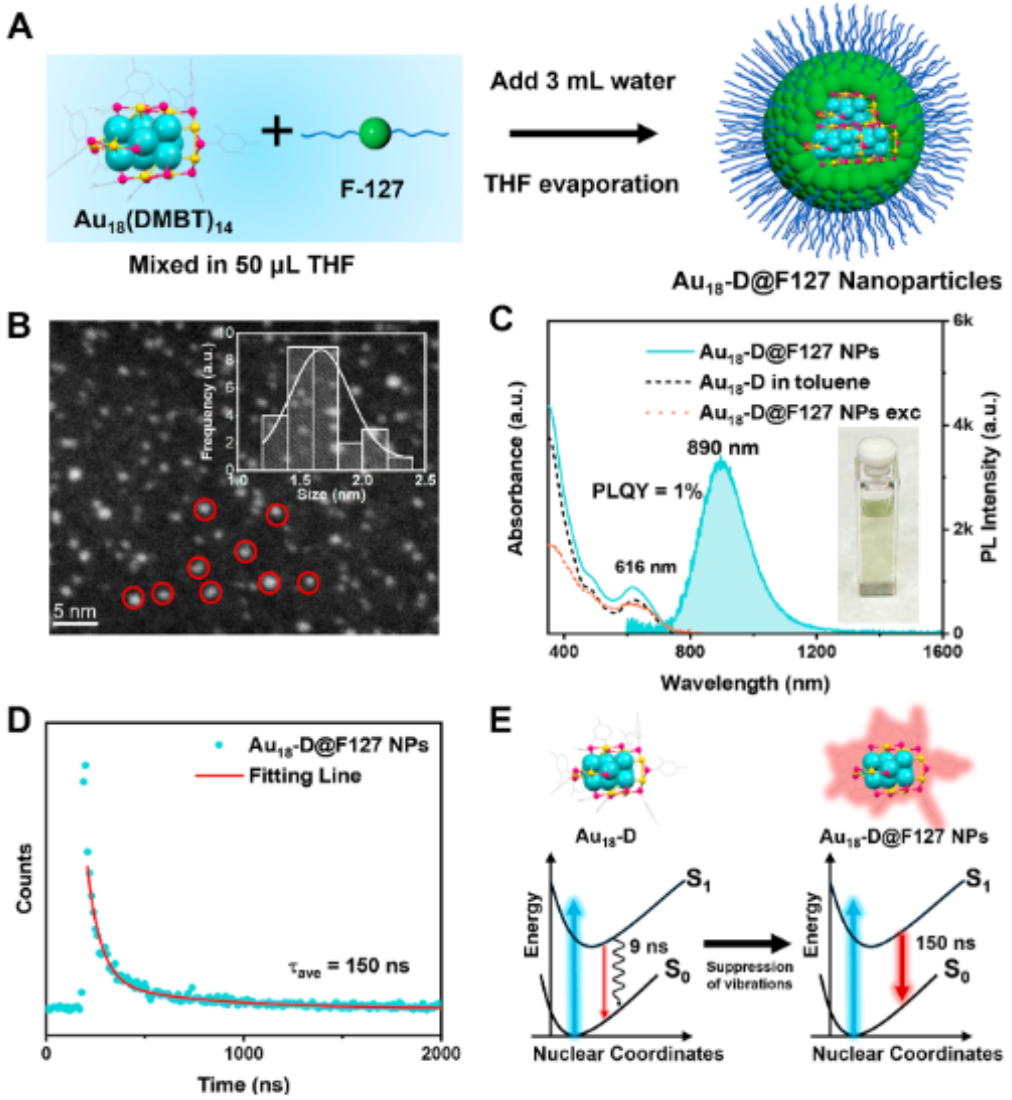

Figure 2. (A) Schematic formation process of Au_{18}-D@F127 NPs. (B) Scanning transmission electron microscopy (STEM) image of Au_{18}-D@F127 NPs and their size distribution (shown in the inset). (C) Absorption (solid line) and PL (shaded area) spectra of Au_{18}-D@F127 NPs in deaerated D_2O (with N_2). The dashed black line is the absorption spectrum of Au_{18}-D in toluene. The dotted red line is the excitation spectrum for PL at 890 nm. (For PL measurements: excitation at 400 nm with 0.2 optical density (OD), slit width 8 nm, and emission slit 8 nm.) (D) PL decay curve of Au_{18}-D@F127 NPs in D_2O (the red line is the fitting result). (E) Schematic illustration of excited-state dynamics of Au_{18}-D and Au_{18}-D@F127 NPs.

Generizability

Genera

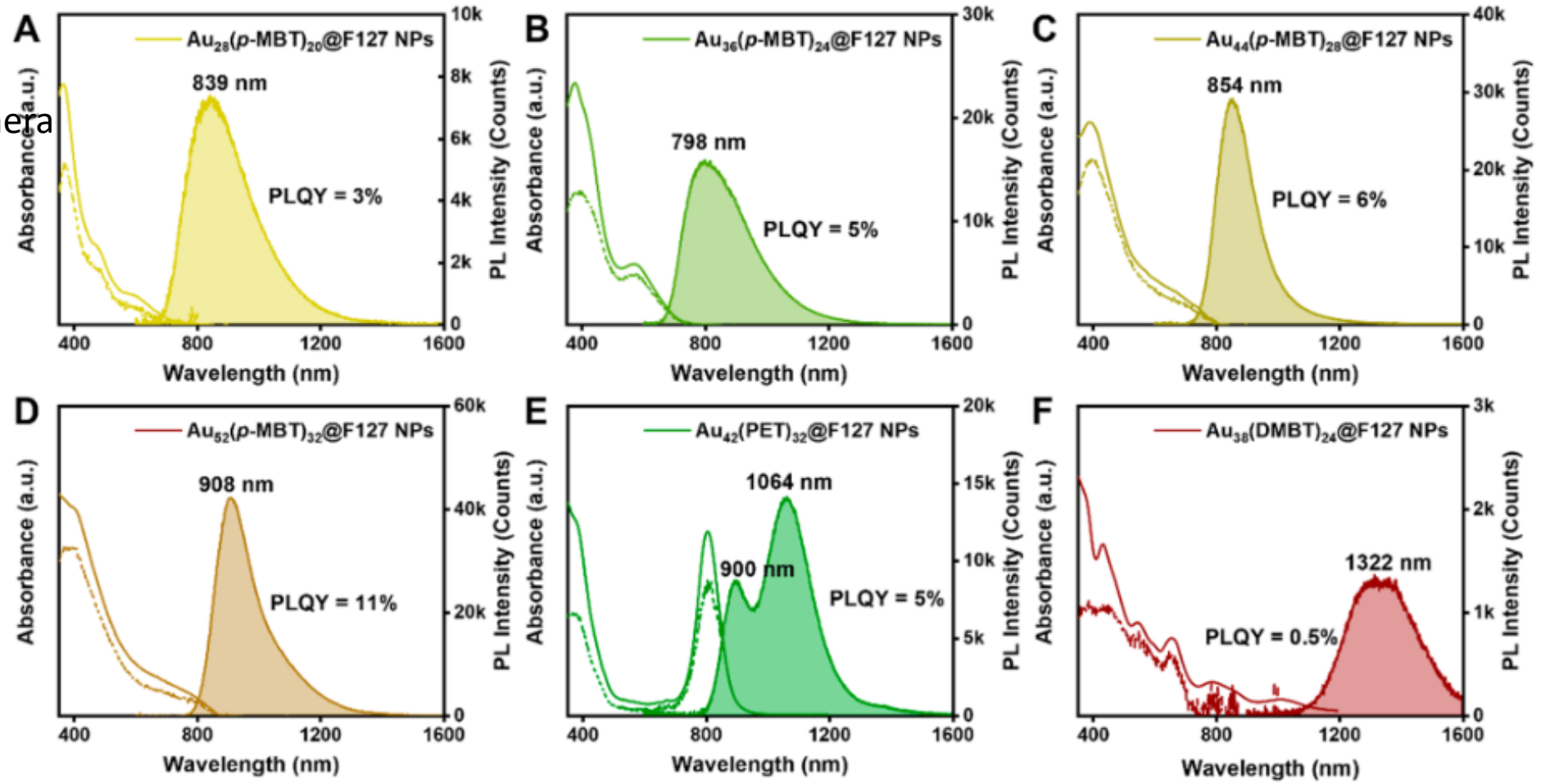

Figure 3. Absorption (solid lines) and PL emission (shaded areas) spectra of F127 wrapped NCs. (A) $Au_{28}(p\text{-MBT})_{20}$, (B) $Au_{36}(p\text{-MBT})_{24}$, (C) $Au_{44}(p\text{-MBT})_{28}$, (D) $Au_{52}(p\text{-MBT})_{32}$, (E) $Au_{42}(PET)_{32}$, and (F) $Au_{38}(DMBT)_{24}$ in deaerated D_2O (with N_2). Dashed lines represent the PL excitation spectra. (For PL measurements: excitation at 400 nm with 0.2 OD, slit width 8 nm, and emission slit 8 nm).

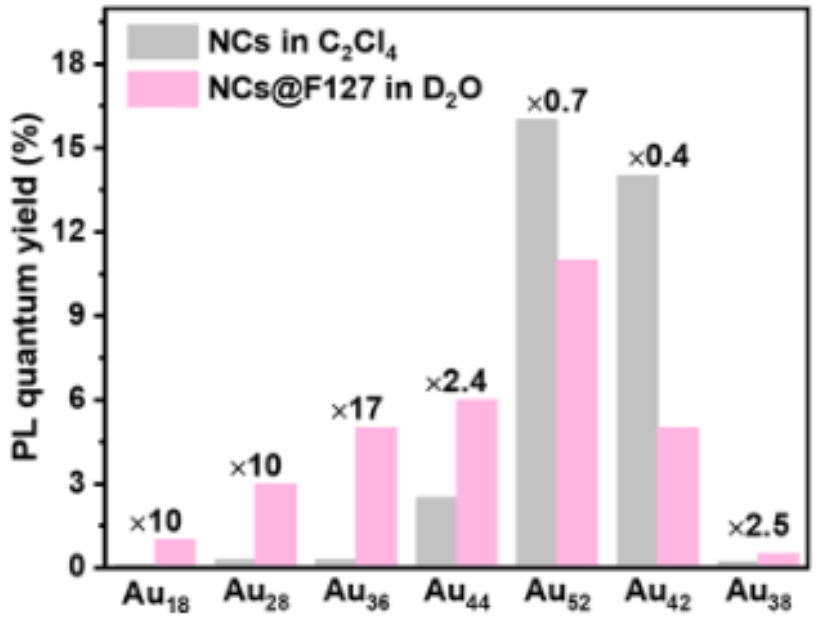

Figure 4. Comparison of PLQY for six NCs in C_2Cl_4 (gray bars) and after transfer into D_2O (pink bars). For Au_{18}, its PLQY in organic solution is very low (~0.1%) and thus barely discernible in the bar graph.

Degradation study of organic pollutants

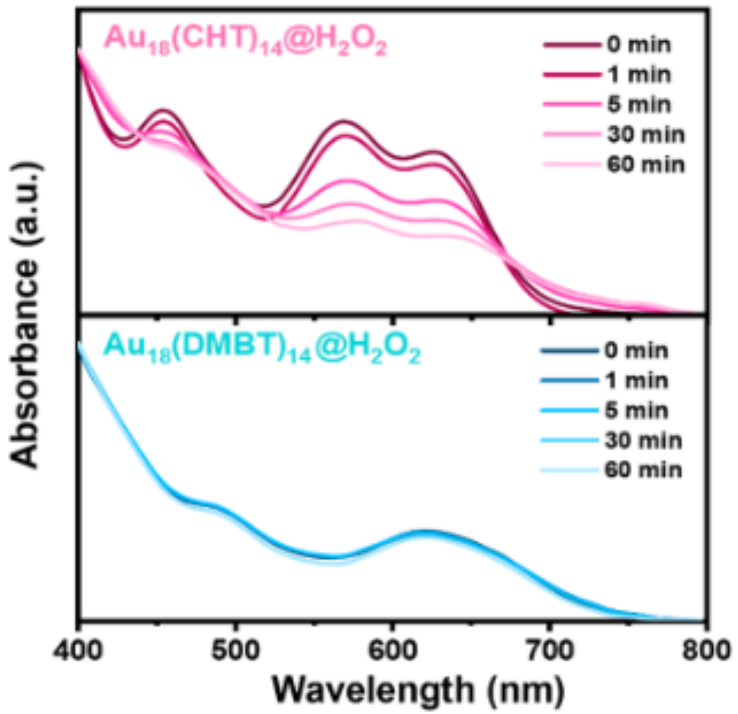

Figure 5. Antioxidation stability of $Au_{18}(CHT)_{14}$ (upper panel) and $Au_{18}(DMBT)_{14}$ (bottom panel) during the treatment with H_2O_2 (monitored by time-dependent optical absorption).

Scheme 1. Photocatalytic Degradation of Organic Pollutants Using Au_{18}-D@F127 Nanoparticles as a Catalyst

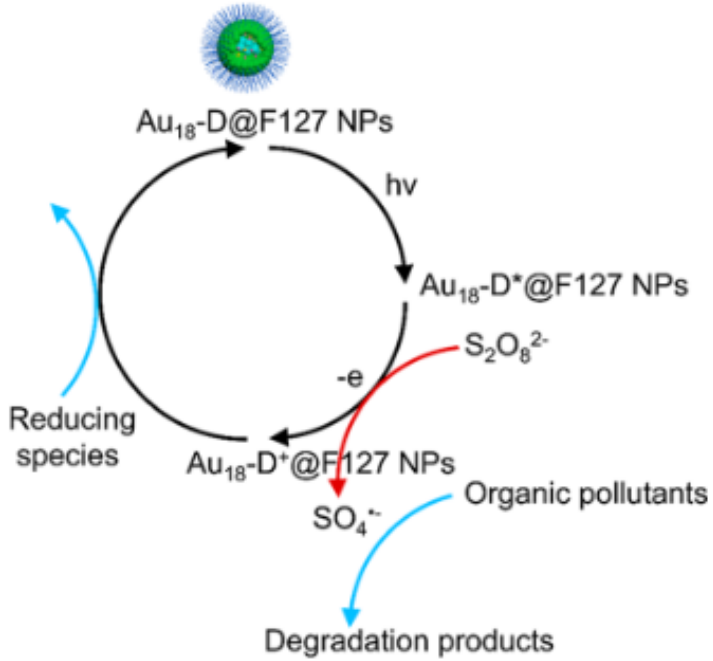

(DV 51)

5 W 650 nm red LED

$k = 0.02\ min^{-1}$

CBZ

8 W 365 nm

$0.12\ min^{-1}$

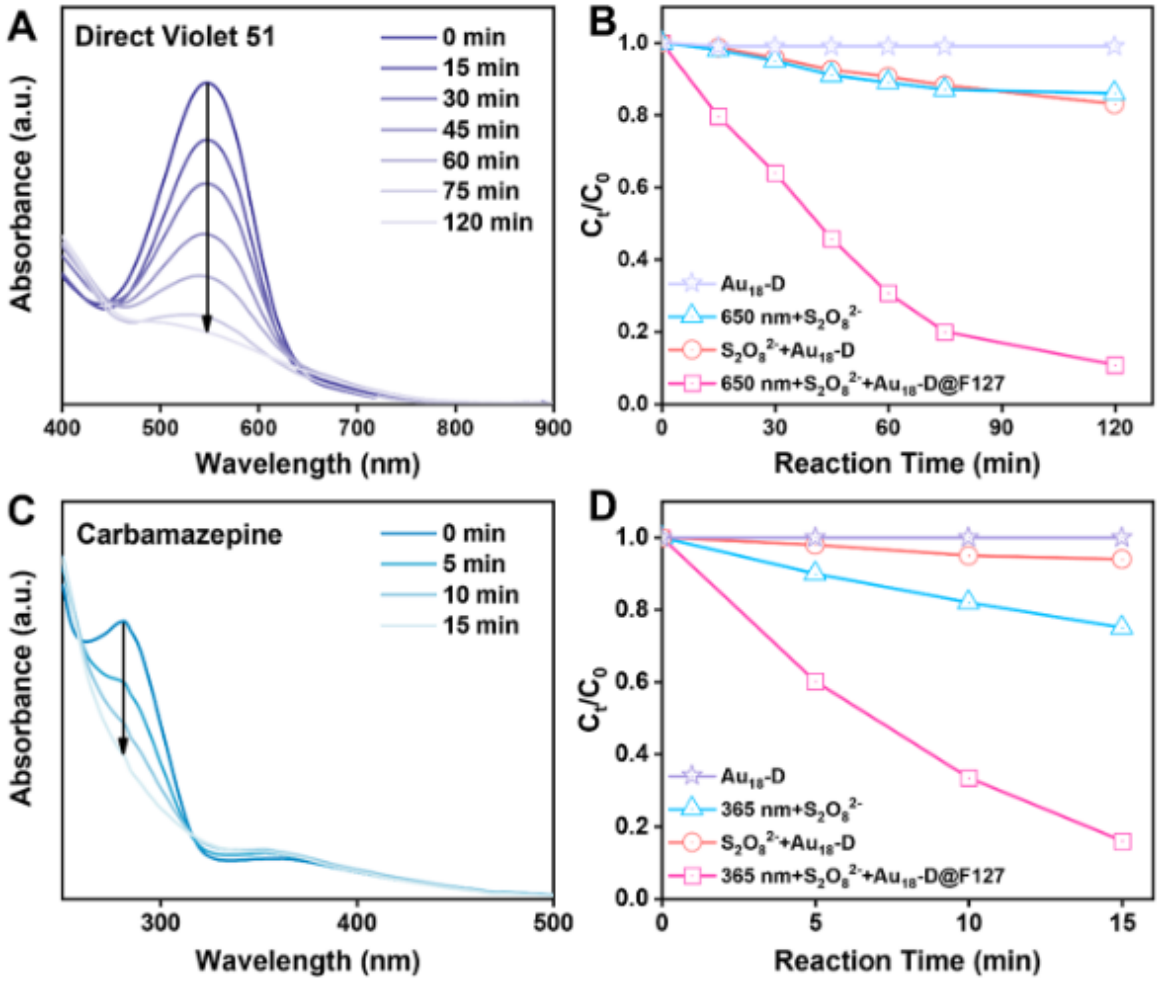

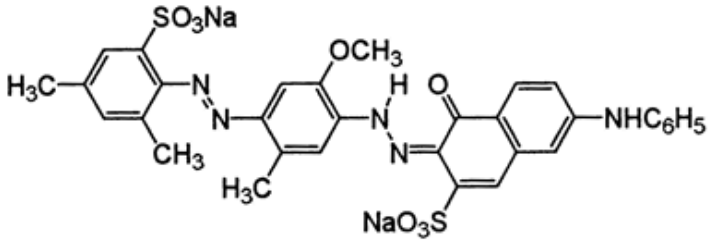

Direct Violate 51

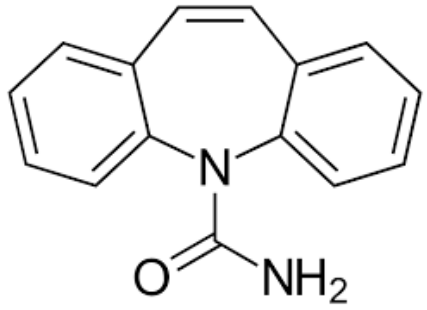

Carbamazepine

Figure 6. (A) UV−vis spectra of DV51 during photocatalytic degradation. (B) Comparison of photocatalytic degradation efficiency of DV51 with various control groups (data adapted from panel A). (C) UV−vis spectra of CBZ during photocatalytic degradation. (D) Comparison of photocatalytic degradation efficiency of CBZ with various control groups (data adapted from panel C).

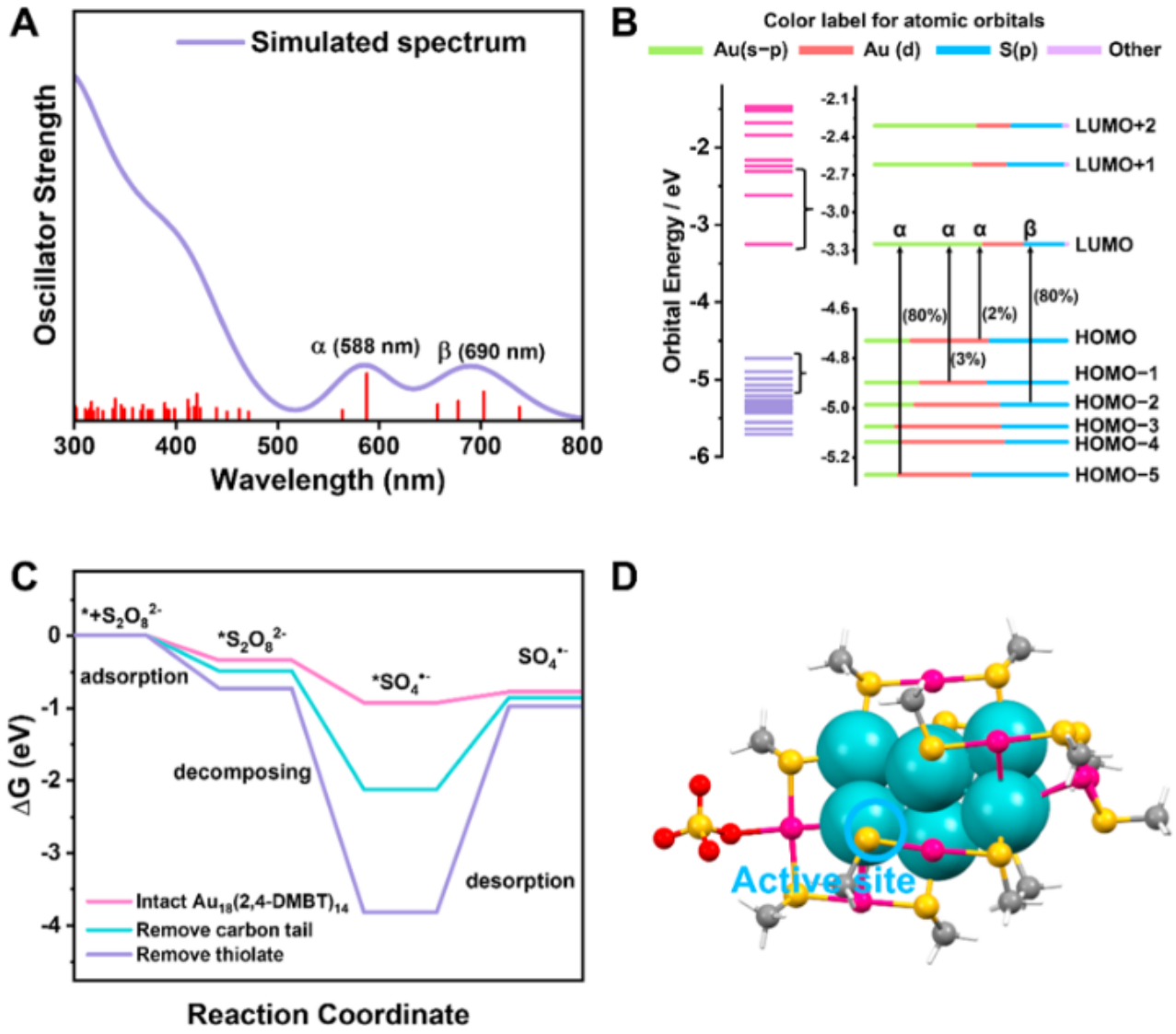

Figure 7. (A) Time dependent DFT-simulated absorption spectrum of $Au_{18}(SCH_3)_{14}$. (B) Kohn−Sham (KS) orbital energy level diagram of $Au_{18}(SCH_3)_{14}$. (C) Calculated free energy profile for the $S_2O_8^{2-}$ to $SO_4^{\bullet-}$ process on $Au_{18}(SCH_3)_{14}$. The asterisk (*) represents the adsorption sites. (D) DFT-simulated catalytic active site on $Au_{18}(SCH_3)_{14}$ for the activation of $*S_2O_8^{2-}$ to form $*SO_4^{\bullet-}$.

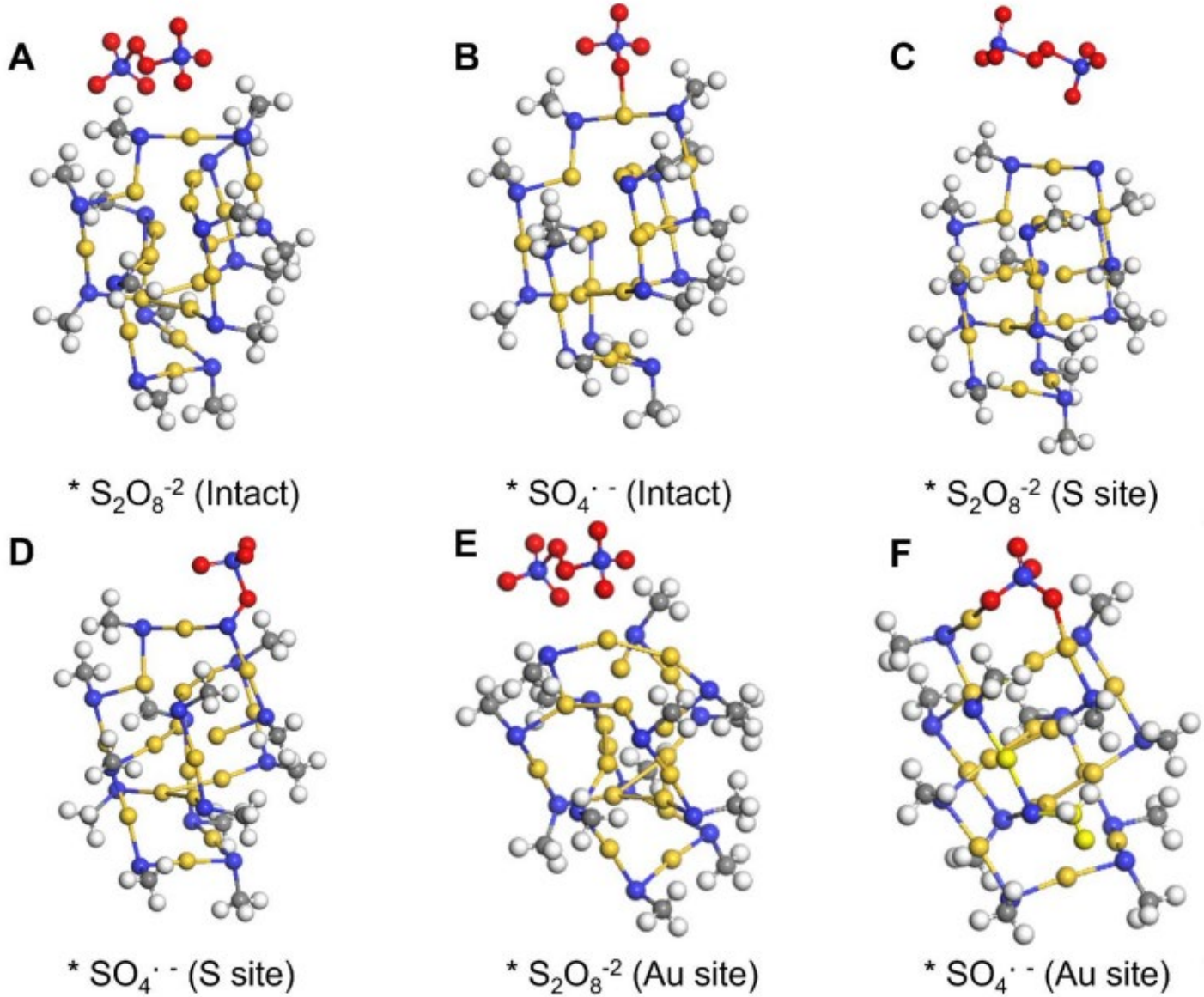

Figure S13. The adsorption and dissociation model of $S_2O_8^{2-}$ ion on intact Au_{18} NC (**A** and **B**), S site (**C** and **D**), and Au site (**E** and **F**).